0026-895X/02/6101-43–54$3.00
MOLECULAR PHARMACOLOGY
Vol. 61, No. 1
1142/951366
*Mol Pharmacol* 61:43–54, 2002
*Printed in U.S.A.*


# A Novel Class of Peptides with Facilitating Action on Neuronal Nicotinic Receptors of Rat Chromaffin Cells in Vitro: Functional and Molecular Dynamics Studies

SILVIA DI ANGELANTONIO, VALERIA COSTA, PAOLO CARLONI, LUIGI MESSORI, and ANDREA NISTRI

*Biophysics (S.D.A., V.C., A.N.) and Condensed Matter Sectors (P.C.) and Istituto Nazionale per la Fisica della Materia Unit (S.D.A., V.C., P.C., A.N.), International School for Advanced Studies, Trieste, Italy; and Department of Chemistry, University of Florence, Firenze, Italy (L.M.)*

Received June 7, 2001; accepted September 21, 2001

This paper is available online at http://molpharm.aspetjournals.org

## ABSTRACT

Peptides related to the N-terminal region of calcitonin gene-related peptide (CGRP) were tested for their ability to modulate neuronal nicotinic acetylcholine receptors (nAChRs) of rat cultured chromaffin cells under whole cell patch-clamp conditions. Although $CGRP_{1-7}$ and $CGRP_{2-7}$ depressed responses mediated by nAChRs, $CGRP_{1-6}$, $CGRP_{1-5}$, or $CGRP_{1-4}$ rapidly and reversibly potentiated submaximal nicotine currents while sparing maximal currents. $CGRP_{1-3}$ was inactive. The threshold concentration for the enhancing effect of $CGRP_{1-6}$ was 0.1 $\mu$M. $CGRP_{1-5}$ or $CGRP_{1-4}$ were less effective than $CGRP_{1-6}$. Coapplication of $CGRP_{1-6}$ and of the allosteric potentiator physostigmine (0.5 $\mu$M) gave additive effects on nicotine currents. $CGRP_{1-6}$ did not enhance responses generated by muscle-type nicotinic receptors of cultured myoblasts or by $\gamma$-aminobutyric $acid_A$ receptors expressed by human embryonic kidney cells. Molecular dynamics (MD) simulations suggested that $CGRP_{1-7}$ exhibited a relatively rigid ring structure imparted by the disulfide bridge between $Cys_2$ and $Cys_7$. The circular dichroism (CD) spectrum recorded from the same peptide was in agreement with this result. Shorter peptides, missing such a bridge, exhibited propensity for $\alpha$-helix configuration. Replacing $Cys_7$ with Ala yielded $CGRP_{1-7A}$, a fragment with partial $\alpha$-helix structure and ability to enhance nicotine currents. CD measurements on $CGRP_{1-6}$ were compatible with these MD structural findings. Short terminal fragments of CGRP represent a novel class of substances with selective, rapid, and reversible potentiation of nAChRs.

Neuronal nicotinic acetylcholine receptors (nAChRs) belong to a family of ACh-gated cationic channels consisting of different subtypes with distinct anatomical distribution in the vertebrate central and peripheral nervous systems (for reviews, see Role and Berg, 1996; Gotti et al., 1997; Lindstrom, 1997; Paterson and Nordberg, 2000). Current interest in nAChRs has been prompted by their apparent involvement in a large number of neuropsychiatric disorders such as Alzheimer's disease, Parkinson's disease, epilepsy, and schizophrenia (for a recent review, see Paterson and Nordberg, 2000). Despite their different causes and pathogeneses, these diseases share a common neurochemical deficit: loss or dysfunction of nAChRs. Hence, the identification of chemicals that can selectively potentiate responses mediated by nAChRs is clearly a major goal to develop potential therapeutic drugs. So far, two main classes of compounds have been used for this purpose: cholinesterase inhibitors, which prevent breakdown of endogenous ACh and thus lead to a build up of this transmitter at the receptor level (Maelicke and Albuquerque, 2000), and allosterically potentiating ligands (APLs) of nAChRs, which enhance ACh interaction with its receptors (Maelicke et al., 1997; Krause et al., 1998). Although these substances have been shown to induce clinical benefit (Maltby et al., 1994; Nordberg et al., 1998; Sjoberg et al., 1998), either approach has some pitfalls. First, these compounds are not entirely selective for nAChRs. Second, their use may lead to receptor desensitization caused by persistent activation of nAChRs. Third, some agents, such as APLs, possess a relatively narrow range of pharmacological effectiveness and can actually block nAChRs if used at doses not much higher than the potentiating ones.

Using nAChRs of rat chromaffin cells as a model system, we have reported that the 1 to 7 N-terminal fragment of

This work was supported by a grant from Ministero dell'Università e della Ricerca Scientifica e Tecnologica (to A.N.) and by Istituto Nazionale per la Fisica della Materia.

**ABBREVIATIONS:** nAChR, neuronal nicotinic acetylcholine receptor; ACh, acetylcholine; APL, allosterically potentiating ligand; $CGRP_{1-x}$, 1 to *x* N-terminal fragment of calcitonin gene-related peptide, where x is 3, 4, 5, 6, or 7; HEK, human embryonic kidney; GABA, $\gamma$-aminobutyric acid; BAPTA, 1,2-bis(2-aminophenoxy)ethane-*N*,*N*,*N*′,*N*′-tetraacetic acid; $CGRP_{1-7A}$, N-terminal fragment of calcitonin gene-related peptide in which $Cys_7$ is replaced by Ala; $CGRP_{2-7}$, N-terminal fragment of calcitonin gene-related peptide missing $Ser_1$; CD, circular dichroism; TFE, trifluorethanol; $R_G$, radius of gyration; MD, molecular dynamics.

calcitonin gene-related peptide ($CGRP_{1-7}$) behaves as a potent antagonist of nAChRs (Giniatullin et al., 1999). The composition of rat chromaffin cell nAChRs is not clear, although in bovine chromaffin cells, $\alpha3(\alpha5)\beta4$ subunits are the main constituents (Campos-Caro et al., 1997). It is noteworthy that rat chromaffin cells do not possess $\alpha7$ receptors as indicated by their lack of $\alpha$-bungarotoxin-sensitive binding sites and absence of $\alpha$-bungarotoxin antagonism of fast nAChR-mediated responses (Khiroug et al., 1997; Di Angelantonio et al., 2000). Because in the adrenal medulla CGRP is present in nerve fibers (Costa et al., 1994; Heym et al., 1995) and in the chromaffin cells themselves (Kuramoto et al., 1987), modulation of nAChRs by the native peptide (and perhaps even by its fragments in case of any significant cleavage by peptidases) might be of physiological significance.

In the attempt to identify the minimal amino acid sequence retaining this antagonist action, we decided to investigate the effects of shorter fragments of this peptide, namely, $CGRP_{1-6}$, $CGRP_{1-5}$, $CGRP_{1-4}$, and $CGRP_{1-3}$. To our surprise, some of these compounds exhibited a powerful potentiating action on nAChRs. The present report thus comprises a functional characterization of this unexpected phenomenon and molecular dynamics studies of these peptides to identify some structural requirements that may impart either potentiating or antagonist properties to these molecules. The MD calculations were supported by circular dichroism measurements. Our structural investigation led to the synthesis of a substituted peptide endowed with receptor-potentiating effects.

## Experimental Procedures

### Cell Preparation for Electrophysiology

Adrenal medulla were removed from 25- to 35-day-old rats (anesthetized with slowly rising levels of $CO_2$) and rinsed in a medium, pH 7.2, containing 137 mM NaCl, 3 mM KCl, 0.7 mM $Na_2HPO_4$, 25 mM HEPES, 10 mM glucose, and 350 units/ml penicillin and streptomycin. Chromaffin cells were dissociated by treating adrenal tissue fragments and cultured at 37°C for 1 to 2 days under a 5% $CO_2$-containing atmosphere as described previously (Khiroug et al., 1998; Di Angelantonio et al., 2000). I28 cells in culture were prepared as described by Irintchev et al. (1997). HEK 293 cells were transfected with $\alpha1\beta2\gamma2$ $GABA_A$ receptors as previously reported (Granja et al., 1998).

### Patch-Clamp Recording

Cell-containing culture dishes (used at 0–3 days from plating) were mounted on the stage of an inverted Nikon Diaphot microscope and superfused (5–10 ml/min) with control saline solution containing 135 mM NaCl, 3.5 mM KCl, 1 mM $MgCl_2$, 2 mM $CaCl_2$, 15 mM glucose, and 10 mM HEPES (pH adjusted to 7.4 with NaOH; osmolarity, 285 mOsM). Patch pipettes pulled from thin glass had 5- to 6-MΩ resistance when filled with 120 mM CsCl, 20 mM HEPES, 1 mM $MgCl_2$, 3 mM $Mg_2ATP_3$, and 10 mM BAPTA (240 mOsM). The pH of the pipette solution was always adjusted to 7.2 with CsOH. Unless otherwise indicated, cells were voltage clamped at −70 mV. After obtaining whole cell configuration, a 10-min period of stabilization normally elapsed before membrane currents were recorded, filtered at 1 kHz, and acquired on the hard disk of a PC by means of pCLAMP 6.04 software (Axon Instruments, Foster City, CA).

### Drugs and Application Method

A series of peptides related to the N-terminal sequence of CGRP were custom synthesized by Neosystem (Strasbourg, France). These are listed in Fig. 1 and include $CGRP_{1-7}$ and its derivatives $CGRP_{1-7A}$ (in which $Cys_7$ was replaced by Ala) and $CGRP_{2-7}$ (with missing $Ser_1$), $CGRP_{1-6}$, $CGRP_{1-5}$, $CGRP_{1-4}$, and $CGRP_{1-3}$. nAChRs of chromaffin cells are particularly prone to desensitization, which develops with a fast time constant of 110 ± 20 ms (Khiroug et al., 1998), thus ruling out attainment of steady-state responses with applications of nicotine lasting even 1 s only. This property makes it very difficult to use standard methods for agonist application to construct dose-response curves under equilibrium conditions and to express meaningful quantitative values in terms of drug receptor occupancy on intact cells. To circumvent this problem, agonists were usually delivered by pressure application (10–20 psi) from glass micropipettes positioned about 15 to 25 μm away from the recorded cell (Giniatullin et al., 2000). We have recently reported, with experimental and theoretical data, an approach to quantify the pressure application method in terms of actual drug concentration applied to single cells (Di Angelantonio and Nistri, 2001). For this purpose, we compared, on the same cells, the inward currents generated by applying nicotine via a pressure pipette or via a PC-controlled rapid solution exchanger (BioLogic, Strasbourg, France) consisting of a

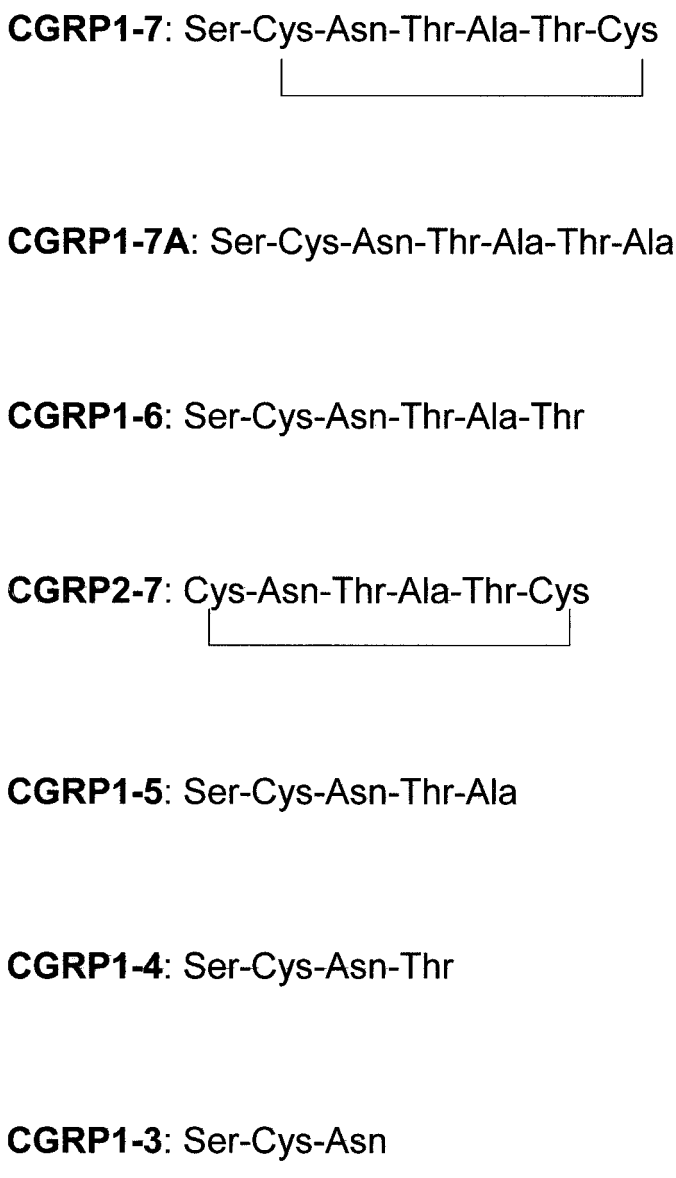


**Fig. 1.** Linear amino acid structure of the peptides $CGRP_{1-7}$ (note disulfide bond), $CGRP_{1-7A}$, $CGRP_{2-7}$, $CGRP_{1-6}$, $CGRP_{1-5}$, $CGRP_{1-4}$, and $CGRP_{1-3}$.

multibarrelled array of glass tubes (1 mm o.d.) rapidly rotating to generate a stream of solution to the recorded cell. With the rapid solution system, the shortest application time was 1 s, to avoid significant dilution of the agonist concentration inside the glass tubes by their capillarity backfilling from the bath (this problem does not apply to pressure pipettes with narrow orifices of about 3 $\mu$m in diameter). We then compared equiamplitude peak responses induced with the two different application methods whenever they were reproducible and without fading (indicative of desensitization). We observed that with the typical puffer pipette concentration (100 $\mu$M nicotine), the largest agonist concentration reaching the cell membrane was 92 $\mu$M and was attained after 117 ms. For shorter nicotine pulses (usually in the 5–100-ms range), a standard pulse lasting, for example, 20 ms would yield 42 $\mu$M concentration at membrane level 30 ms later (corresponding to the peak of nicotine current). Intermediate pulses generated an average 2.3-fold agonist dilution, a value close to the nearly 3-fold dilution calculated with a different method based on changes in junction potentials in the absence of cells (Giniatullin et al., 1996). These results indicate that, to obtain reliable responses due to nAChR activity, the pressure application method was a simple approach yielding responses in which receptor desensitization was minimized.

Parallel tests were also performed to validate the effects of peptides on responses to puffer-applied agonists by repeating experiments with the rapid superfusion system. In this case nicotine and the peptide fragment were rapidly coapplied via glass barrels and gave results analogous to those found with the puffer application of nicotine (see *Results*; Fig. 2). Note that the limited number of barrels that the rotating head assembly could carry restricted the number of drug concentrations in combination with the agonist to be tested on each cell. This method was therefore unsuitable to explore, in quantitative manner, a broad concentration range of test compounds. Conversely, fast superfusion of antagonists or modulators (which per se did not have any agonist activity) was a convenient approach to apply such substances (within a small range of known concentrations), whereas agonists were applied via puffer pipettes.

## Electrophysiological Data Analysis

Data are presented as mean ± S.E.M. ($n$ is number of cells) with statistical significance assessed with Wilcoxon test (for nonparametric data) or paired $t$ test (for normally distributed data). A value of $P \leq 0.05$ was accepted as indicative of a statistically significant difference. Dose-response curves were fitted with a standard logistic equation (Sokolova et al., 2001); zero for the fit was set when there was no agonist or current.

## Circular Dichroism Spectroscopy

CD spectra were obtained at 20°C under a constant flow of nitrogen by a Jasco J715 spectropolarimeter, which was calibrated with an aqueous solution of ammonium D-camphorsulfate. Experimental measurements were carried out in aqueous or aqueous/trifluoroethanol (TFE) solutions by using a 1-mm path-length cuvette. CD spectra of the free peptides were recorded in the UV region (190–250 nm). Peptide concentration was around 0.3 mg/ml. Spectra represent the average of four scans. CD intensities are expressed as mean residue ellipticities (degree $cm^2 \cdot mol^{-1}$) calculated by $\theta = \theta/lcn$, where $\theta$ is the ellipticity observed (degrees), $l$ is the pathlength of the cuvette (cm), $c$ is the peptide concentration (M), and $n$ is the number of amino acids in the peptide.

## Computational Methods

**Structural Models.** We examined four CGRP terminal fragments (Fig. 1): 1) $CGRP_{1–7}$, in which $Cys_2$ and $Cys_7$ form a disulfide bridge; 2) $CGRP_{1–7A}$, which is the same as $CGRP_{1–7}$ except that Ala replaced $Cys_7$; 3) $CGRP_{1–6}$; and 4) $CGRP_{1–5}$. The initial structural model of $CGRP_{1–7}$ was built through a systematic search of the Protein Data Bank for a protein containing a ring of six amino acids closed up by a disulfide bridge. We selected the X-ray structure of progastricsin (Moore et al., 1995; entry 1HTR, www.rcsb.org/pdb/index.html, because its residues $Cys_{45}$-$Gln_{46}$-$Ser_{47}$-$Gln_{48}$-$Ala_{49}$-$Cys_{50}$ form a six-membered disulfide ring. These residues were found to display a very good Ramachandran plot (Ramachandran and Saiekharan, 1968), indicative of a highly plausible spatial conformation of this protein. To build the $CGRP_{1–7}$ model, we replaced $Gln_{46}$,

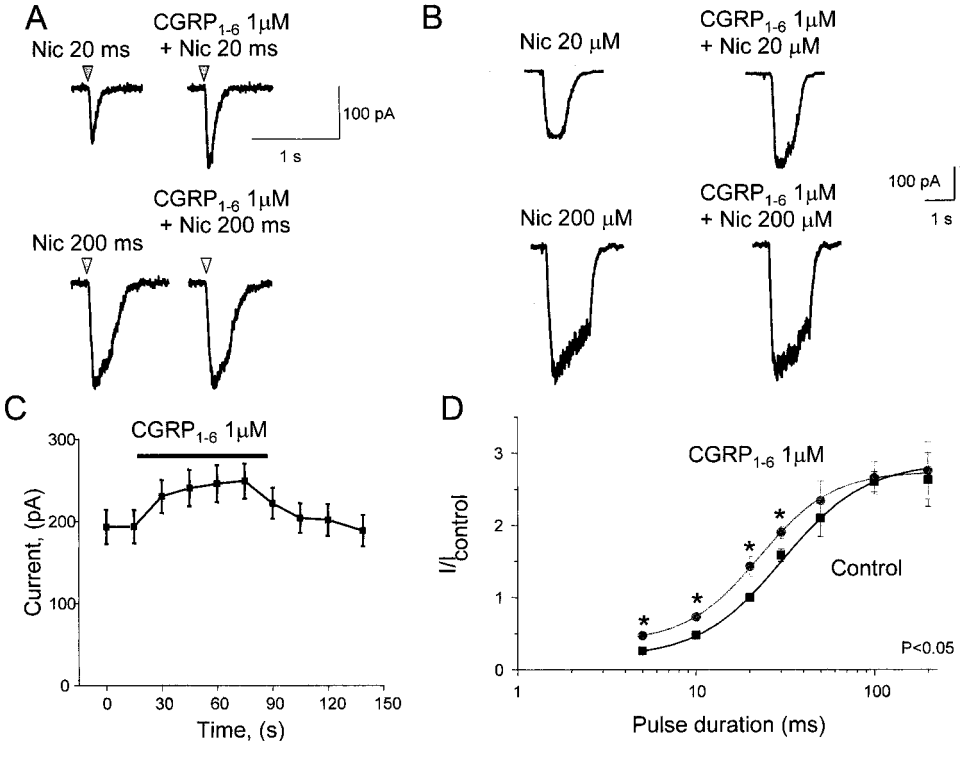


**Fig. 2.** Effect of $CGRP_{1–6}$ on nicotine-evoked currents. A, top, submaximal currents induced by a short, nonsaturating nicotine pulse (20 ms) are potentiated by this peptide fragment, whereas maximal currents (200-ms nicotine pulse) are not affected (bottom). B, current response to superfusion of 20 $\mu$M nicotine together with $CGRP_{1–6}$ (1 $\mu$M) is enhanced with respect to control (top), whereas maximum response to 200 $\mu$M nicotine is unaffected by 1 $\mu$M $CGRP_{1–6}$ (bottom). C, time course of the $CGRP_{1–6}$ action on nAChR: currents elicited by nicotine are rapidly potentiated and this effect is reversible after 45 to 60 s of washout. D, dose-response curve (expressed as pulse duration versus response) for nicotine in control and in the presence of $CGRP_{1–6}$ (1 $\mu$M); the plot in the presence of the peptide is shifted to the left in a parallel manner without altering maximal responses ($n$ = 5–12). Currents are normalized with respect to response to 20-ms pulse in control solution and fitted with the logistic equation. *, $P < 0.05$.

$Ser_{47}$, $Gln_{48}$, and $Ala_{49}$ with Asn, Thr, Ala, and Thr, respectively. A Ser residue was attached to $Cys_{45}$; $NH3^+$ and $COO^-$ terminal groups were added. The initial models of $CGRP_{1-7A}$, $CGRP_{1-6}$, or $CGRP_{1-5}$ were constructed as follows. A linear structure (i.e., backbone dihedral angles $\Phi = \Psi = 180°$) was first constructed. A simulated annealing procedure similar to that of Daura et al. (1998) was then performed in three steps: 1) for each peptide molecular dynamics simulations at 1000 K temperature were first carried out for 10 ps; 2) eight structurally different conformers, selected from this simulation, were cooled from 600°K to 0.5°K in 1.5 ns; and 3) the lowest-energy models were finally used for the molecular dynamics simulation in water.

The computational setup was the same as the one described in the section below, except that no periodic boundary conditions and no cutoff for electrostatic interactions were used. The four CGRP terminal fragments simulated in a water cubic box of about 30 $Å^3$ were further studied as indicated below.

**Computational Setup.** The AMBER (Cornell et al., 1995; http://www.amber.ucsf.edu/amber/) or TIP3P (Jorgensen et al., 1983) force fields were used to describe the interatomic potential energy functions of peptides or water, respectively. The dielectric constant was set to 1. The time-step integration of the Newton equation of motion was set to 1.5 fs. Temperature (298°K) and pressure (1 bar) were kept constant by coupling the peptide/water systems to a Berendsen bath algorithm (Berendsen et al., 1984) with 1.0-ps relaxation time. van der Waals interactions were truncated up to a spherical, residue-based cut-off of 12 Å. Periodic boundary conditions (Allen and Tildesley, 1987) were imposed to avoid problems due to the small dimensions of the system. Electrostatic interactions were calculated using the Ewald particle mesh method (Essmann at al., 1995).

**Molecular Dynamics Calculations.** The simulation procedure was carried out as follows. First, the solvent underwent energy minimization and was equilibrated (with a molecular dynamics process) with the peptide for 30 ps at constant volume. Subsequently, the entire system was heated from 0° to 298°K for 0.12 ns at 1 bar pressure. Finally, 10-ns molecular dynamics simulations at 298°K temperature and 1 bar pressure were performed. All calculations were carried out with the SANDER module of the AMBER5 suite of programs running on a four-processor SGI Origin 200 parallel machine (SGI, Mountain View, CA). Ten-nanosecond simulation for each peptide required approximately 20 days of calculations.

**Calculated Properties.** Data for the last 9 ns of molecular dynamics simulations were collected for analysis. The radius of gyration ($G_R$) of the peptide backbone atoms was calculated, taking as a reference the atom position at 1 ns. $G_R$ was calculated as

$$\frac{1}{nr}\sqrt{\frac{1}{N}\sum_{i=1}^{N}(r_i - r_G)^2}$$

where $nr$ is the number of residues, $N$ is the number of steps (about 2000) for which averages were calculated, $r_i$ is the position vector of all backbone atoms at step $i$, and $r_G$ is the position vector of the mass center.

Ramachandran plots were calculated using the Procheck program (Laskowski et al., 1993; http://www.biochem.ucl.ac.uk/~roman/procheck/procheck.html). $\alpha$-Helix conformations were assigned based on the $\Phi$ and $\psi$ backbone torsion angles.

## Results

### Potentiation of Nicotine-Evoked Responses by $CGRP_{1-6}$

Figure 2A shows inward currents generated by nicotine (applied via brief pressure pulses from a 0.1 mM pipette concentration to minimize rapid desensitization; Khiroug et al., 1997) from a chromaffin cell in culture. When a 20-ms pulse was delivered in the presence of $CGRP_{1-6}$ (1 $\mu$M; applied by rapid superfusion), the inward current was unexpectedly potentiated (53%; Fig. 2A, top). This phenomenon was not associated with any direct action of $CGRP_{1-6}$ on resting conductance or baseline current, indicating that this substance did not have agonist activity on nAChRs or nonspecific actions on membrane leak channels. On the same cell, $CGRP_{1-6}$ (1 $\mu$M) was ineffective on 200-ms pulse nicotine currents (Fig. 2A, bottom), which were large enough to reach the responsiveness plateau (Giniatullin et al., 1999). Figure 2B shows effects observed when nicotine or nicotine plus $CGRP_{1-6}$ were both applied via the fast superfusion system. Again, the inward current induced by 20 $\mu$M nicotine was potentiated by coapplied $CGRP_{1-6}$ (1 $\mu$M; 39% potentiation), whereas the maximal current elicited by 200 $\mu$M nicotine was unaffected by the peptide. On average, $CGRP_{1-6}$ enhanced currents to 20 $\mu$M nicotine by 33 ± 8% ($n = 5$; $P < 0.05$). Previous experiments have indicated that semilog plots of pressure pulse/current responses were linear within the 10- to 50-ms application range and corresponded very closely to those produced by superfusing 20 to 100 $\mu$M nicotine (Di Angelantonio and Nistri, 2001), suggesting the upper and lower concentration limits reached with puffer application.

The $CGRP_{1-6}$ effect was manifested already with the first nicotine response elicited just 5 s after starting peptide superfusion, and was reversible after 1 min of washout (Fig. 2C; $n = 11$). The rapid action of $CGRP_{1-6}$ was also confirmed by the fact that, when coapplied with nicotine, it immediately increased nicotine currents as long as the responses were submaximal (Fig. 2B).

Further tests were performed to characterize the action of $CGRP_{1-6}$ (1 $\mu$M). Figure 2D shows that the plot relating inward current amplitude to the amount of nicotine (expressed as millisecond application; Giniatullin et al., 1999) with plateau value at 100-ms pulse ($n$ = 5–12 cells). When comparable applications were repeated in the presence of 1 $\mu$M $CGRP_{1-6}$ (15-s preapplication), inward currents induced by 5- to 30-ms nicotine pulses were significantly ($P < 0.05$) potentiated, whereas responses induced by 50- to 200-ms pulses were unaffected. Thus, the plot was shifted to the left in an apparently parallel manner while retaining analogous maximum response. $CGRP_{1-6}$ (1 $\mu$M) thus enhanced nicotine responses at approximately mid-point of the curve (20 ms) by 31 ± 7% ($n = 30$). These data, therefore, demonstrate that the potentiating action of $CGRP_{1-6}$ was dependent on the amount of agonist delivered to the cell.

Figure 3A shows the concentration dependence (0.05–100 $\mu$M range) of $CGRP_{1-6}$ effects on nAChRs activated by a fixed dose of nicotine (20 ms; 0.1 mM): potentiation had threshold at 0.1 $\mu$M (5 ± 7%; $n = 7$; $P < 0.05$) and reached an apparent maximum at 50 $\mu$M (56 ± 6%; $n = 5$; $P < 0.05$). Note that, as indicated by Fig. 2D, this "dose" of puffer-applied nicotine induced membrane current amplitudes approximately one-half of the apparent maximum (Di Angelantonio and Nistri, 2001). The $CGRP_{1-6}$ potentiating action was also present when cytisine rather than nicotine was the test agonist (20 ms; 0.1 mM; Fig. 3B), as also indicated by the superimposed plots for the potentiation by $CGRP_{1-6}$ toward nicotine- or cytisine-evoked currents (Fig. 3B, inset). The slope values for the nicotine or cytisine plots of Fig. 3, A and B, were 1.1 ± 0.02 and 1.02 ± 0.02, respectively. These results thus demonstrate that nAChR facilitation by $CGRP_{1-6}$ was agonist-

independent. The $CGRP_{1-6}$-potentiating action was independent also from membrane potential, as shown in Fig. 3C, in which average current responses from six cells held at −40, −70, or −100 mV are compared.

Although these experiments showed an interesting potentiating action of $CGRP_{1-6}$, they did not clarify whether this was specific for nAChRs. To this end we studied whether this peptide possessed similar effects also on muscle-type nicotinic receptors of I28 cells in culture (these are primary myoblasts; Irintchev et al., 1997; Wernig et al., 2000). On these cells (clamped at −60 mV holding potential) superfusion of nicotine (0.1 mM, which was the $EC_{50}$ concentration) evoked average responses of 1.06 ± 0.22 nA peak ($n$ = 7), readily reversible after washout. When nicotine was applied in the continuous presence of 1 μM $CGRP_{1-6}$ (preapplied for 2 min), evoked currents did not change in amplitude (1.09 ± 0.24 nA, which corresponded to 101 ± 2% of controls; $n$ = 7; data not shown). Further tests were conducted to find out whether distinct ionotropic receptors gated by other transmitters, for instance, GABA, could also be affected by $CGRP_{1-6}$ (1 μM). For this purpose, we recorded inward currents generated by 3-ms application of 1 mM GABA to HEK 293 cells ($n$ = 6) expressing $\alpha1\beta2\gamma2$ $GABA_A$ receptors (Granja et al., 1998). $CGRP_{1-6}$ did not change (101 ± 1%) responses to GABA, indicating that its action was not present on muscle-type AChRs and was not generalized to ionotropic neuronal receptors.

### Interaction between $CGRP_{1-6}$ and $CGRP_{1-7}$

The potentiation by $CGRP_{1-6}$ is in sharp contrast with the depression of nicotine-evoked currents induced by $CGRP_{1-7}$ (Giniatullin et al., 1999). Loss of a single amino acid thus transformed the biological activity of the peptide fragment. Which of the two effects on nAChRs would prevail if these compounds were applied simultaneously? This issue was tested in experiments similar to those reported in Fig. 3D. The average potentiation due to $CGRP_{1-6}$ was 31 ± 7% ($n$ = 30) and the mean depression due to $CGRP_{1-7}$ was 42 ± 11% ($n$ = 17). Coapplication of 0.5 μM $CGRP_{1-6}$ plus 1 μM $CGRP_{1-7}$ depressed (by 34 ± 3%; $n$ = 5) the 20-ms nicotine-induced submaximal currents, whereas coapplication of the same peptides at equimolar concentration (1 μM) left nicotine responses unchanged (99 ± 4%; $n$ = 9). When 1 μM $CGRP_{1-6}$ plus 0.5 μM $CGRP_{1-7}$ was applied, the nicotine currents were significantly enhanced by 16 ± 6% ($n$ = 5). These results suggest that these peptide fragments were apparently equipotent in exerting their modulatory action, although of diametrically opposite direction.

### Effect of $CGRP_{1-5}$, $CGRP_{1-4}$, or $CGRP_{1-3}$ Fragments

How conserved is the enhancing action of $CGRP_{1-6}$? This question was addressed by studying the effects of the shorter fragments $CGRP_{1-5}$, $CGRP_{1-4}$, or $CGRP_{1-3}$. Figure 4A shows that $CGRP_{1-5}$ significantly potentiated 20-ms nicotine-induced currents in a concentration-dependent manner. However, this facilitation was less pronounced than the one exerted by $CGRP_{1-6}$. In fact, although $CGRP_{1-6}$ (1 μM) potentiated by 31 ± 7% ($n$ = 30), $CGRP_{1-5}$ (1 μM) potentiated by 20 ± 4% only ($n$ = 8). To obtain a comparable degree of potentiation (26 ± 4%) it was necessary to use a 10-fold higher concentration of $CGRP_{1-5}$ (10 μM; $n$ = 5). Further increases in $CGRP_{1-5}$ concentrations (50–100 μM) did not augment the extent of potentiation (Fig. 4A).

The fragment $CGRP_{1-4}$ (1 μM) also displayed a slight, yet significant, potentiating effect (8 ± 1%; $n$ = 14), whereas at 10 μM concentration, it significantly potentiated by 18 ± 3% ($n$ = 6). $CGRP_{1-3}$ (1 or 10 μM) did not alter nicotine-induced currents (0 ± 1%; $n$ = 7). These data are summarized in Fig. 4B, in which the action of the various CGRP fragments is compared with the one of the native peptide (all compounds tested at 1 μM concentration).

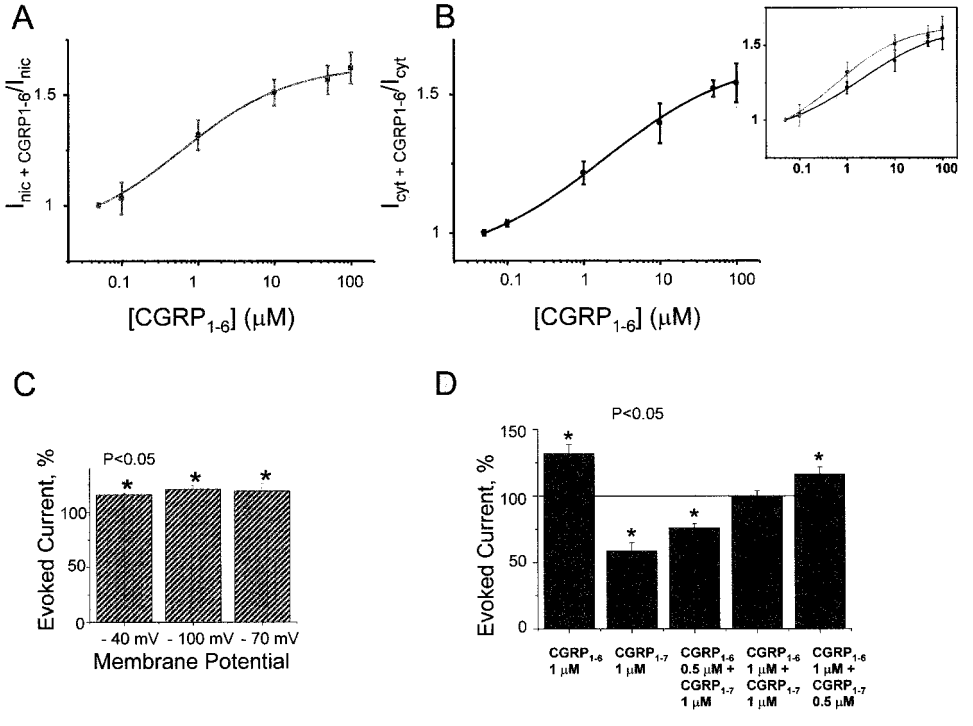


**Fig. 3.** Analysis of the mechanism of action of $CGRP_{1-6}$. A, nicotine current potentiation (0.1 mM; 20 ms) at different $CGRP_{1-6}$ concentrations; the threshold for potentiation is 0.1 μM; the same behavior is shown in B with cytisine as test agonist (0.1 mM; 20 ms). Abscissa: $CGRP_{1-6}$ concentrations (log units); ordinate: current ratio in $CGRP_{1-6}$ ($I_{nic+CGRP}$ or $I_{cyt+CGRP}$) over the one in control solution ($I_{nic}$ or $I_{cyt}$). Inset, superimposed plots for nicotine and cytisine responses, indicating similar shape. C, histograms demonstrating the equi-amplitude increase in 20-ms nicotine-evoked currents (expressed as percentage of control) at the three holding membrane potentials indicated below columns. Each column is significantly different from control (*, $P < 0.05$; $n$ = 7). D, comparison of the action of $CGRP_{1-6}$ or $CGRP_{1-7}$ or a mixture of the two on 20-ms nicotine currents. Note that the potentiation due to $CGRP_{1-6}$ is canceled by the competitive antagonism exerted by $CGRP_{1-7}$ when the two peptides are applied together. All responses are expressed as ratio of nicotine-evoked currents in the presence of the peptides with respect to control ($n$ = 6).

### Comparison between $CGRP_{1-6}$ and a Typical Allosterically Potentiating Ligand

The unusual action by $CGRP_{1-6}$ on nAChRs raised the possibility that this substance might belong to the category of APLs. These drugs bind to a discrete site of nAChRs from which they allosterically up- or down-regulate the action of nicotinic agonists (Maelicke et al., 1997; Changeux and Edelstein, 1998; Maelicke and Albuquerque, 2000). APLs often produce a biphasic action such that, in low doses, they facilitate agonist responses, whereas in higher doses they depress them. One example of an APL is physostigmine that at the concentration of 0.5 $\mu$M maximally enhances nAChRs via allosteric modulation, whereas at higher concentrations, it actually inhibits them (Maelicke et al., 1997). In the present investigation, we first tested whether this action of physostigmine was also present on native nAChRs of chromaffin cells. To this end, nicotine (20-ms pulse) was applied in the presence of either a small (0.5 $\mu$M) or a high (5 $\mu$M) concentration of physostigmine. Figure 5A shows sample traces demonstrating that 0.5 $\mu$M physostigmine potentiated nicotine-induced responses (on average 28 $\pm$ 5%; $n$ = 14), whereas 5 $\mu$M depressed them (on average 48 $\pm$ 2%; $n$ = 4). Figure 5B shows the nicotine dose-response curve in control solution or in the presence of 0.5 $\mu$M physostigmine ($n$ = 4–14 cells). Physostigmine shifted the plot to the left, which attained a larger (85 $\pm$ 5%) maximal response ($P < 0.01$). These data confirm that physostigmine acted on nAChRs of chromaffin cells with a pharmacological profile typical of an APL and quite distinct from that of $CGRP_{1-6}$ (Fig. 2). These observations led us to study whether $CGRP_{1-6}$ and physostigmine had distinct action on nAChRs. For this purpose, on a sample of five cells, standard responses induced by 20-ms nicotine were first potentiated, by the same degree, by $CGRP_{1-6}$ (1 $\mu$M) or physostigmine (0.5 $\mu$M) applied separately (21 $\pm$ 4 or 20 $\pm$ 6% potentiation, respectively; Fig. 5C). We then coadministered these two substances while testing currents produced by 20-ms nicotine puffs. In the latter case, the potentiation was 37 $\pm$ 6%, which is a value near the sum of the two individual effects (Fig. 5C).

Conversely, when the physostigmine concentration was

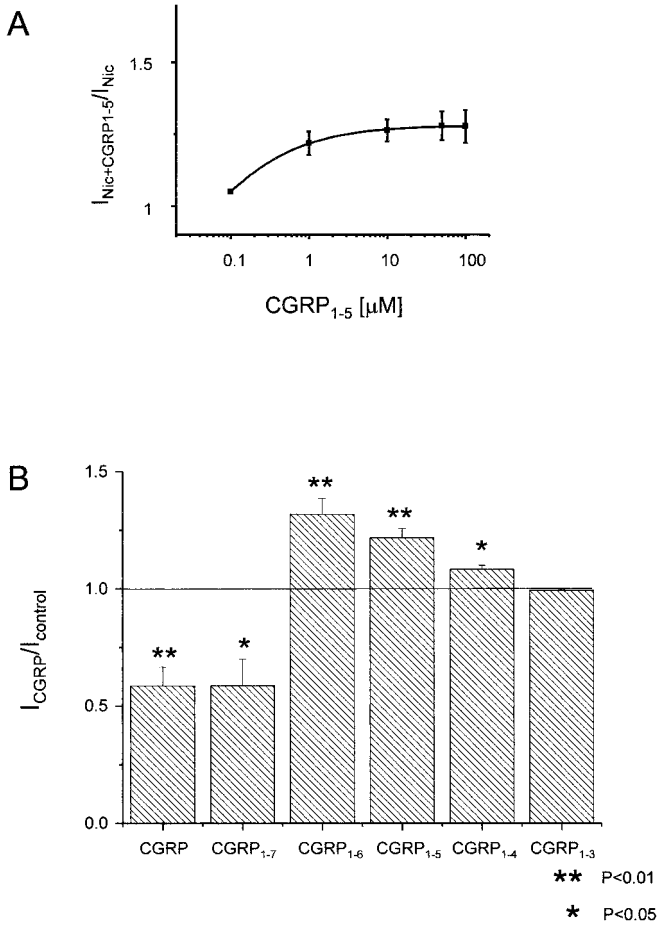


**Fig. 4.** Effect of $CGRP_{1-5}$, $CGRP_{1-4}$, and $CGRP_{1-3}$ fragments on nAChRs. A, concentration dependence of potentiation of nicotine currents by $CGRP_{1-5}$. B, histograms summarizing the action of different fragments of CGRP (all compounds applied at 1 $\mu$M concentration) on nicotine-mediated responses. The efficacy of $CGRP_{1-5}$ is less than the one observed with the 1 to 6 fragment. $CGRP_{1-4}$ maintains a slight potentiating effect, whereas $CGRP_{1-3}$ is inactive. For comparison, data corresponding to the antagonism exerted by CGRP and $CGRP_{1-7}$ are reported. Responses are expressed as ratios of currents in the presence of CGRP or its fragment ($I_{CGRP}$) with respect to controls.

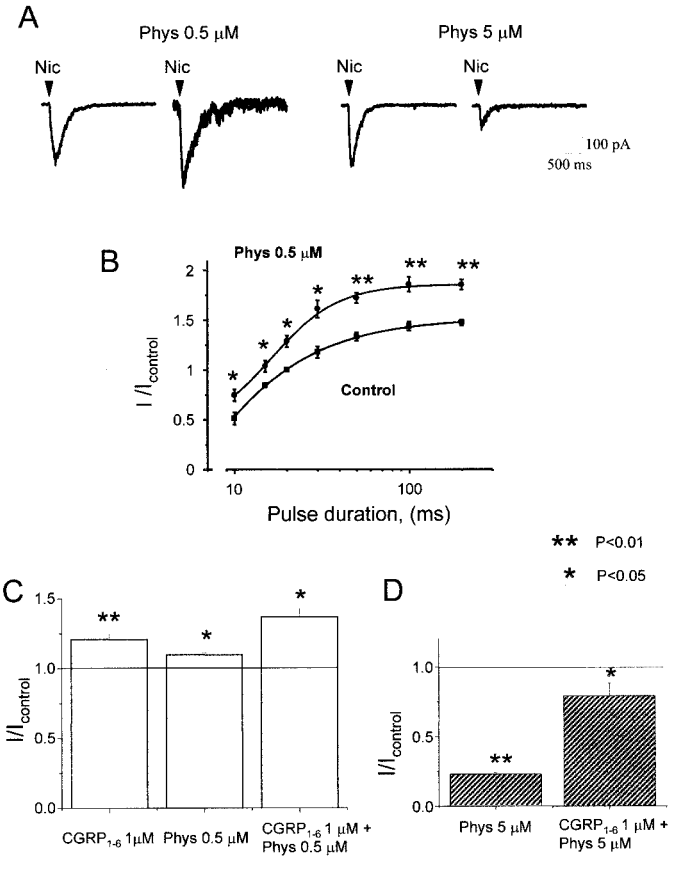


**Fig. 5.** Interaction between $CGRP_{1-6}$ and physostigmine (Phys). A, on the same cell, a small concentration (0.5 $\mu$M) of physostigmine potentiates nicotine-induced currents (0.1 mM; 20 ms), whereas a higher one depresses them (5 $\mu$M). B, nicotine dose-response curve (0.1 mM) in control and in the presence of physostigmine (0.5 $\mu$M; $n$ = 4–14). Physostigmine potentiates all nicotine-mediated responses, including the maximal one. C, histograms summarizing the action on 20-ms nicotine-induced currents by $CGRP_{1-6}$ (1 $\mu$M) or physostigmine (0.5 $\mu$M) applied either separately or simultaneously. Asterisks indicate level of significance ($n$ = 5). D, Histograms showing the depressant action of physostigmine (5 $\mu$M) on nicotine-evoked responses and the opposing action by subsequent application of $CGRP_{1-6}$ (1 $\mu$M; $n$ = 4). Responses to nicotine are expressed as ratio between the current in the presence of the drug (I) and in control solution ($I_{control}$).

higher (5 $\mu$M), nicotine-induced currents became 23 ± 1% of the control amplitude (Fig. 5D). In this case, adding $CGRP_{1-6}$ (1 $\mu$M) could partly counteract the inhibition caused by physostigmine because the nicotine-evoked responses were 79 ± 1% of the control amplitude (Fig. 5D; $n = 4$). These results indicate that the action of $CGRP_{1-6}$ on nAChRs took place whether these were enhanced or inhibited by physostigmine.

### Effect of $CGRP_{1-7A}$ or $CGRP_{2-7}$ Fragments

Why did deletion of a single amino acid from $CGRP_{1-7}$ convert a depressant action into a potentiating one? Inspection of the primary amino acid sequences in Fig. 1 shows that absence of Cys from position 7 removed the disulfide bridge linking two cysteines in position 2 and 7. Assuming that removal of the disulfide bridge by deleting $Cys_7$-mediated switching of $CGRP_{1-7}$ from receptor antagonist to receptor enhancer, we predicted that a seven amino acid chain similar to the one of $CGRP_{1-7}$ but lacking a cyclic structure should yield an AChR-potentiating peptide. This hypothesis was tested by replacing $Cys_7$ with Ala, thus yielding a new fragment termed $CGRP_{1-7A}$ (Fig. 1). Figure 6A shows that $CGRP_{1-7A}$ potentiated (+18%) the nicotine (20 ms)-evoked current, and that this effect was reversible after 1 min of washout. The time course of the $CGRP_{1-7A}$ action on nicotine-induced responses is depicted in Fig. 6B: this potentiation was rapid in onset, reached apparent steady-state conditions (maximum potentiation = 17 ± 4%; $n = 8$), and was readily reversible during washout. Figure 6C shows the nicotine dose-response curve in control solution and in the presence of 1 $\mu$M $CGRP_{1-7A}$ (15-s preapplication; $n = 4-8$ cells). In the presence of this peptide inward currents induced by 5- to 50-ms nicotine pulses were significantly ($P < 0.05$) potentiated, whereas responses induced by 100- to 200-ms pulses were unaffected. Thus, the plot was shifted to the left in an apparently parallel manner but retained analogous maximum response.

Further insight into the structure-activity relation of these peptides was sought by deleting $Ser_1$ from $CGRP_{1-7}$, thus converting this peptide into a shorter fragment, which nevertheless retained the disulfide bridge (Fig. 1). Figure 6D shows that 1 $\mu$M $CGRP_{2-7}$ reversibly depressed (by 43%) the current response to 20-ms nicotine. The plot of Fig. 6E indicates that the depressant action by $CGRP_{2-7}$ toward 20-ms nicotine currents was concentration-dependent (within the 0.1–10 $\mu$M range). Hence, the $CGRP_{2-7}$ retained (albeit weakly) the depressant action of the longer compound $CGRP_{1-7}$ because at 1 $\mu$M concentration, $CGRP_{1-7}$ and $CGRP_{2-7}$ inhibited nicotine currents by 45 ± 5% (Fig. 4B) and 32 ± 8% ($n = 6$; Fig. 6E), respectively.

### Structural Determinants of Peptides in Solution

A major goal of our work was to relate the structural properties of the peptides in solution to their modulatory properties on nAChRs. To this end, we have performed a combination of circular dichroism measurements, which can provide insights into the relative preponderance of various secondary structures for each peptide in solution (Impellizzeri et al., 1998, and references therein), and molecular dynamics, which can provide atomic structural models.

**CD Spectra of $CGRP_{1-7}$ and $CGRP_{1-6}$.** The CD spectra of $CGRP_{1-7}$ and $CGRP_{1-6}$ in aqueous salt solution (containing 25 mM phosphate buffer and 4 mM NaCl at pH 7.4) were significantly different, suggesting underlying dissimilarities in their structure (Fig. 7). Indeed, the spectrum of $CGRP_{1-6}$ (Fig. 7a) showing a negative band peak at 198 nm is diagnostic of an essentially "disordered" conformation; its CD intensity at 220 nm was very low. In contrast, a negative band at 204 nm characterized the spectrum of $CGRP_{1-7}$ (Fig. 7c) with a hump around 220 nm; the band was indicative of some structural organization. Further data were obtained by recording the CD spectra of the two peptides in 50% TFE/water solution. The spectrum of $CGRP_{1-6}$ was largely af-

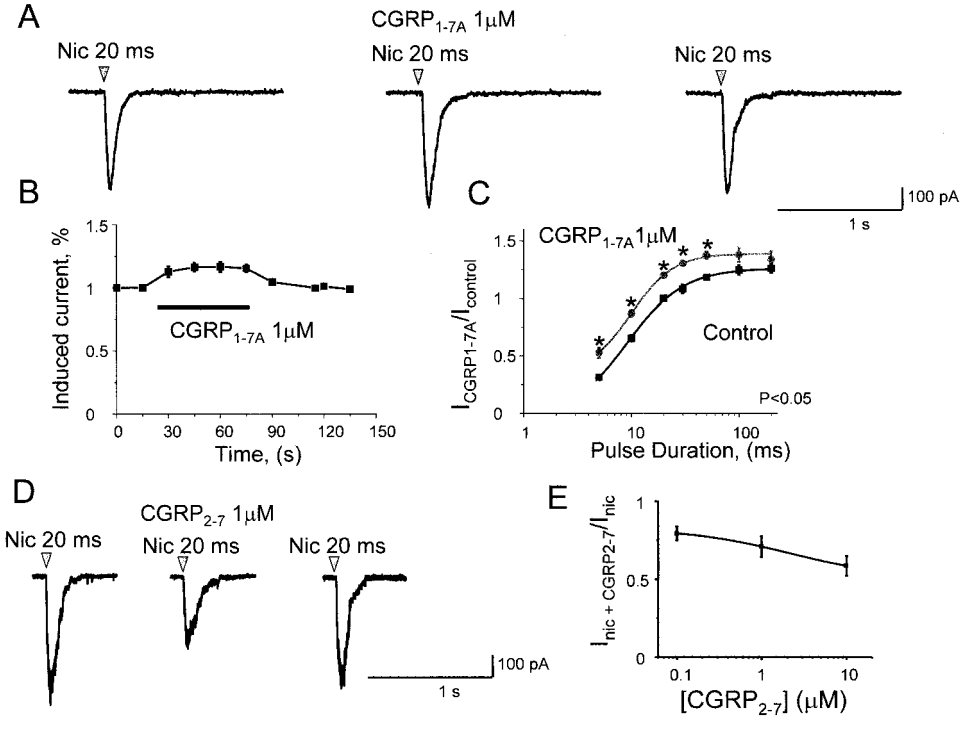


**Fig. 6.** Effect of the $CGRP_{1-7A}$ fragment on nicotine-evoked responses. A, examples of current induced by 20-ms nicotine that is potentiated by 1 $\mu$M $CGRP_{1-7A}$ (preapplied for 15 s). This effect is reversible after peptide washout (right). B, time course of $CGRP_{1-7A}$ potentiation of 20-ms nicotine-induced responses. Note rapid onset of the potentiation that reaches 18% and is rapidly washed out. C, nicotine dose-response curve (doses expressed as pulse duration, ms) in control solution and in the presence of 1 $\mu$M $CGRP_{1-7A}$ ($n = 4-8$ cells). The plot is shifted to the left in an apparently parallel manner without significantly changing maximal response. Asterisks indicate $P < 0.05$. D, example of reversible depression by $CGRP_{2-7}$ (1 $\mu$M) of inward currents induced by 20-ms nicotine. E, log plot of $CGRP_{2-7}$ concentration versus response ratio of currents observed in $CGRP_{2-7}$ solution over control. Data are from six cells.

fected (Fig. 7b) as the negative band was shifted to 202 nm and development of a negative hump around 220 nm appeared. Conversely, the conformation of $CGRP_{1–7}$ in solution was only slightly changed by switching to the TFE/water medium (Fig. 7d).

The CD spectrum of an $\alpha$-helix is characterized by two minima at 222 and 206 nm, and a maximum at 193 nm in solution (Impellizzeri et al., 1998). Thus, any increase in ellipticity absolute values observed at 222 nm when passing from water to a semihydrophobic solvent (50% water/TFE) should indicate larger $\alpha$-helical content of the test samples. Because the random coil conformation generates a very low signal at 222 nm, $CGRP_{1–6}$ has some propensity for helix formation.

**Molecular Dynamics Studies.** In this section the structural properties of the four peptides $CGRP_{1–7}$, $CGRP_{1–6}$, $CGRP_{1–5}$, and $CGRP_{1–7A}$ were investigated in aqueous solution through computer simulations.

*$CGRP_{1–7}$.* Figure 8A shows the structure of this peptide in aqueous solution. A six amino acid ring results from the disulfide bridge (yellow sticks) between $Cys_2$ and $Cys_7$. An inner ring hydrogen bond (Fig. 8A, dashed line) between the backbone carbonyl of $Thr_4$ and the backbone amide of $Cys_7$ was found throughout all dynamics simulation (the distance $d$ between [O($Thr_4$)-NH($Cys_7$)] was 2.4 ± 0.3 Å). The conformation of $CGRP_{1–7}$ backbone was relatively rigid ($R_G$ = 0.75 ± 0.03 Å). Some flexibility was observed on the plane orthogonal to the inner hydrogen bond. Water molecules were not found within the ring. All side chains and carbonyl oxygen atoms were outwardly directed away from the ring.

*$CGRP_{1–6}$.* An H-bond between $Ser_1$ backbone carbonyl oxygen and the Thr4 NH group (Fig. 8B, thick dashed line) was formed after few nanoseconds. Two additional hydrogen bonds [O($Cys_2$)-NH($Thr_6$) and O($Ser_1$)-NH($Ala_5$)] seemed weaker (Fig. 8B, thinner dashed lines) as they broke and immediately reformed several times during the dynamics. The resulting backbone geometry in terms of torsion angles was that of an $\alpha$-helix (Brandsen and Tooze, 1993). The molecular shape was rather flexible ($R_G$ = 0.64 ± 0.05 Å).

*$CGRP_{1–5}$.* As observed with $CGRP_{1–6}$, the $Ser_1$ backbone carbonyl oxygen formed a stable hydrogen bond (Fig. 8C, thick dashed line) with $Ala_5$ ($d$[O($Ser_1$)-NH($Ala_5$)] = 2.8 ± 1.5 Å) after few nanoseconds and a further, albeit weak, hydrogen bond (Fig. 8C, thin dashed line) with $Thr_4$. Consequently, $CGRP_{1–5}$ similarly adopted a rather flexible shape ($R_G$ = 0.66 ± 0.04 Å).

*$CGRP_{1–7A}$.* The hydrogen bond between O($Cys_2$) and NH($Thr_6$) ($d$[O($Cys_2$)-NH($Thr_6$)] = 3.2 ± 0.4 Å; Fig. 8D, thick line) stabilized the $Cys_2$-$Thr_6$ backbone structure. An additional, weak hydrogen bond (Fig. 8D, thin line) between $Asn_3$ carbonyl oxygen and $Ala_7$ formed and broke several times during simulations. Thus, although the $Cys_2$-$Ala_7$ backbone adopted an $\alpha$-helix conformation, the N-terminal residue ($Ser_1$) turned away from the main peptide structure to interact with water. The resulting backbone geometry was rather flexible ($R_G$ = 0.59 ± 0.04 Å).

In conclusion, simulation data highlighted that the AChR-depressant $CGRP_{1–7}$ possessed a ring structure stabilized by a hydrogen bond, whereas the AChR-enhancing peptides preferentially displayed a flexible shape, in which $\alpha$-helix structural elements could be formed and broken during the dynamics.

**Comparison of Peptide Structures.** The ring structure of $CGRP_{1–7}$ set it apart from the other peptides tested in the present study. Instead, $CGRP_{1–6}$, $_{1–5}$, or $_{1–7A}$ conserved the common structural motif of the $\alpha$-helix disclosed by molecular dynamics simulations. However, all these structures turned out to be highly flexible, because most of the H-bond interactions stabilizing the $\alpha$-helical structure were formed and broken several times during the dynamics.

The spatial alignment of $CGRP_{1–6}$ and $CGRP_{1–5}$ (Fig. 9A) suggests that the $CGRP_{1–6}$ structure (blue) was rather similar to that of $CGRP_{1–5}$ (yellow), with only a significant difference in peptide length. By fitting $CGRP_{1–5}$ alongside with the corresponding five amino acids of $CGRP_{1–6}$, it became clear that $CGRP_{1–5}$ had a more extended conformation along the $\alpha$-helical axis (Fig. 9A), possibly because of the lower number of hydrogen bonds between its backbone atoms. $CGRP_{1–6}$ (blue) and $CGRP_{1–7A}$ (magenta) were also rather similar (Fig. 9B): their structures differed only for the conformation assumed by their N-terminal residues, which in the case of $CGRP_{1–6}$ was constrained to the backbone by the two hydrogen bonds.

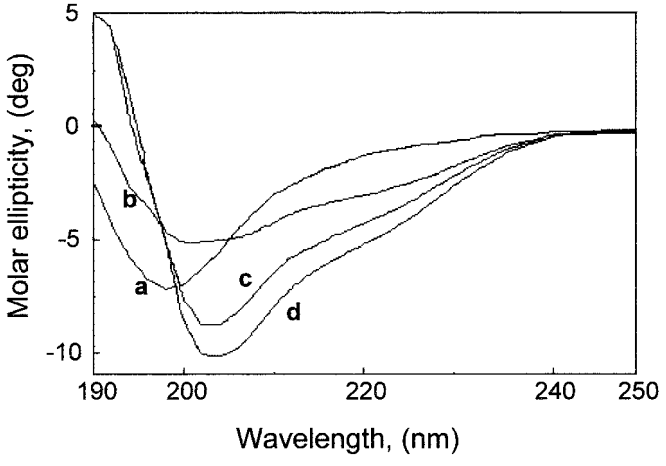


**Fig. 7.** CD spectra of $CGRP_{1–6}$ and $CGRP_{1–7}$ at 20°C. Record of $CGRP_{1–6}$ in phosphate buffer (a), record of $CGRP_{1–6}$ in phosphate buffer/TFE (50/50%) (b), record of $CGRP_{1–7}$ in phosphate buffer (c), and record of $CGRP_{1–7}$ in phosphate buffer/TFE (50/50%) (d).

## Discussion

The principal finding of the present study is the novel, relatively potent modulation by $CGRP_{1–6}$ (and its derivatives) of neuronal nAChRs on rat chromaffin cells: this phenomenon was manifested as a rapid onset and agonist-surmountable potentiation of inward currents evoked by pulse applications of nicotine. Such a potentiation of nicotinic receptors suggests that $CGRP_{1–6}$ and its derivatives are prototypes of a new class of molecules capable of enhancing responses mediated by this class of nAChRs. Further work should be directed to analyze whether the potentiating activity of $CGRP_{1–6}$ (and related compounds) on chromaffin cell nAChRs will be present also on other types of nAChRs commonly found on mammalian central neurons.

**Characteristics of Action of $CGRP_{1–6}$ on Nicotine-Mediated Responses.** When $CGRP_{1–6}$ was superfused onto a chromaffin cell, it evoked no direct change in baseline current or input conductance but it strongly potentiated in-

ward currents induced by nicotine. Potentiation was not use-dependent and was present even with the first response to nicotine in $CGRP_{1-6}$ solution, suggesting that this peptide fragment could have bound nAChRs in the absence of their agonist. The action of $CGRP_{1-6}$ was voltage- and agonist-independent, because responses to cytisine or nicotine were equally increased at various membrane potentials. Note that the slope value for the facilitating action by $CGRP_{1-6}$ was very near 1, suggesting that, within the sensitivity limits of the present technique, there was no apparent heterogeneity of nAChR potentiation or uneven distribution of the peptide. When $CGRP_{1-6}$ was tested on I28 cells, it did not modify responses mediated by muscle nicotinic receptors, indicating specificity of action toward nAChRs present on chromaffin cells. Future work will be necessary to explore the sensitivity of other classes of nAChRs present in the central nervous system to this peptide. It is clear, however, that $CGRP_{1-6}$ was not a nonspecific modulator of ionotropic neuronal receptors because $GABA_A$ receptors were insensitive to it. Therefore, the observed enhancing effects of CGRP fragments were not caused by their interaction with voltage-gated $Ca^{2+}$ or $Na^+$ because cells were routinely voltage clamped at $-70$ mV, a value very far from the voltage threshold for activating those conductances.

**Discrete Changes in Amino Acid Composition of N-Terminal Sequence of CGRP Induced Different Effects on nAChRs.** It was interesting to observe that equimolar concentrations of $CGRP_{1-6}$ and $CGRP_{1-7}$ (Giniatullin et al., 1999), coapplied to the same cell, left nicotine-induced submaximal currents unchanged. This observation suggests that a discrete change in the amino acid sequence, consisting of a single amino acid deletion, could transform an antagonist into a potentiating substance. It seemed thus useful to test whether further reduction in the amino acid sequence length might influence the type of effect on nAChRs. This approach should also help to identify the minimal structure for receptor modulation and to outline some structural characteristics of the peptide molecules that could be exploited with molecular dynamics studies to unveil analogies or differences in spatial conformation.

Deleting one amino acid from the $COO^-$ end of the $CGRP_{1-6}$ sequence clearly yields a compound ($CGRP_{1-5}$) still endowed with potentiating activity on nAChRs (although with reduced potency). Even the $CGRP_{1-4}$ fragment retained a slight, yet significant potentiation, which was lost with $CGRP_{1-3}$. This realization was further examined by analyzing the tridimensional structure of these peptides.

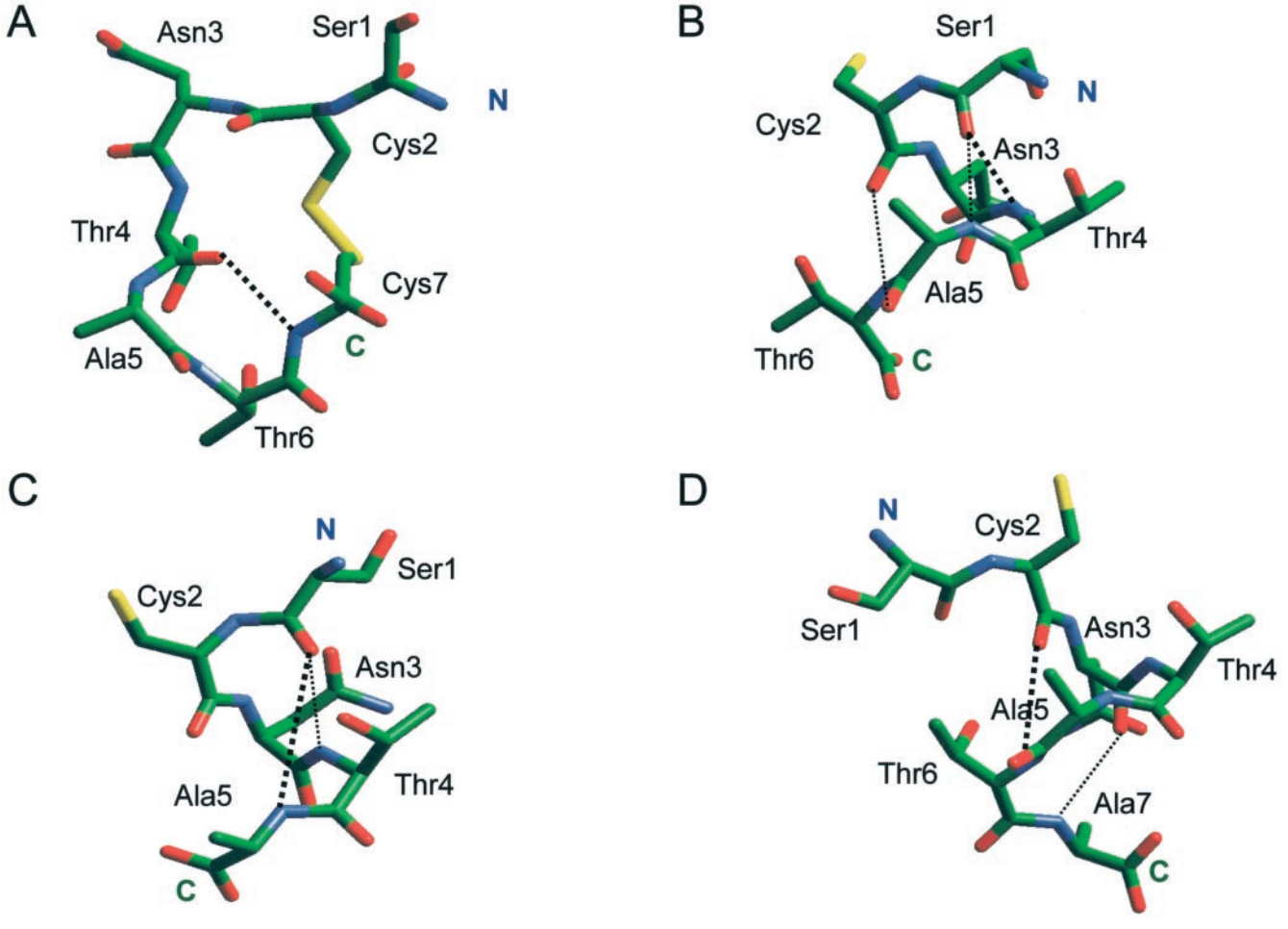


**Fig. 8.** Schematic conformations of the four peptides in aqueous solution as obtained with molecular dynamics calculations. Hydrogen atoms are not displayed for sake of clarity. Hydrogen bonds are indicated as dashed lines of different thickness according to the strength of the bond. $CGRP_{1-7}$ (A), $CGRP_{1-6}$ (B), $CGRP_{1-5}$ (C), and $CGRP_{1-7A}$ (D). Atoms are colored using the following code: oxygen (red), nitrogen (blue) carbon (green) and sulfide (yellow).

**Structure-Function Studies of CGRP Fragments.** Inspection of the linear sequence of the CGRP fragments revealed one major difference between $CGRP_{1-7}$ and $CGRP_{1-6}$, namely, the presence of a disulfide bridge between $Cys_2$ and $Cys_7$, which determined the closed ring structure of $CGRP_{1-7}$. The presence of the disulfide bridge was probably responsible for producing the depressant effect because the shorter fragment $CGRP_{2-7}$ (retaining $Cys_2$ and $Cys_7$) induced antagonism of nicotine responses.

$CGRP_{1-6}$, which was obtained by deleting $Cys_7$, was a more flexible molecule with more freedom to assume various spatial conformations. This realization prompted us to implement further approaches: 1) the synthesis of a seven amino acid peptide analogous to $CGRP_{1-7}$, except that the terminal $Cys_7$ was replaced by Ala and was thus devoid of the disulfide bridge. This new compound, termed $CGRP_{1-7A}$, was observed to behave similarly to its shorter length counterpart $CGRP_{1-6}$ in potentiating nAChRs, although with somewhat reduced potency. 2) CD spectra of two representative peptides ($CGRP_{1-7}$ and $CGRP_{1-6}$) were performed to reveal the presence of secondary structure organization. The CD spectra suggest that the two structures were different, and that $CGRP_{1-7}$ was more rigid than $CGRP_{1-6}$. The latter peptide assumed mostly a random coil conformation. 3) Molecular dynamics simulations were used as a tool to unveil the folding of these novel compounds. In addition, this method should aid detection of conformational analogs, which may provide a structural base for grouping substances so far associated merely by their pharmacological action. Furthermore, understanding the molecular structure of these peptides should help to understand their potential target sites on nAChRs for which substances that are even more powerful might be synthesized in the future.

MD simulations indicated that the ring structure of $CGRP_{1-7}$ was stabilized by an inner ring hydrogen bond. This interaction ensured a rather rigid structure, in agreement with CD results. This rather rigid structure was presumably responsible for blocking agonist binding to nAChRs and was indeed the molecular determinant of the antagonist activity of the native CGRP itself (Giniatullin et al., 1999).

$CGRP_{1-6}$, $CGRP_{1-5}$, and $CGRP_{1-7A}$ turned out to be structurally similar and preferentially adopted a flexible structure, partly with an $\alpha$-helix conformation. Most of the H-bond interactions stabilizing the secondary structure motif were lost and reformed within the time scale investigated.

Our molecular modeling suggests a larger propensity for helix formation than the one indicated by CD measurements performed on one of these peptides ($CGRP_{1-6}$). This discrepancy may be ascribed to the different time scales investigated because MD simulations analyzed nanosecond domains, whereas CD spectra obtained averaged structures over 50 to 200 s. Thus, the MD sampling might have been predominantly oriented to a certain conformation present in water solution: a highly flexible $\alpha$-helix. A small amount of such a conformation (10 to 15%) is indeed compatible with the CD results (Reed and Reed, 1997).

On the basis of CD data the propensity of $CGRP_{1-6}$ for $\alpha$-helix formation increased when the solvent was changed from water to a semihydrophobic one (TFE/water). This result suggests that at the level of the nAChR binding site, which is expected to be a low dielectric medium, the population of $\alpha$-helix structures might become relevant for biological responses. Therefore, the helical conformations of $CGRP_{1-6}$, $CGRP_{1-5}$, and $CGRP_{1-7A}$, obtained with MD simulations, may be of special interest to interpret peptide-receptor interactions. Perhaps this conformation is important for enhancing the action of the agonist on nAChRs but is itself devoid of any direct activity on the agonist binding site. However, due to limited sampling of MD simulations, it is difficult to relate detailed structural properties of these peptides to their affinity toward nAChRs.

**Insights into Mechanism of Action of $CGRP_{1-6}$.** Whereas the present structure-function studies suggested some properties that may account for the receptor-modulating activity of these peptides, the precise mechanisms responsible for these effects remain unclear. This is partly due to methodological considerations because the use of nonequilibrium responses to nicotine and the puffer application protocol (to minimize receptor desensitization) precluded strictly quantitative pharmacological data to analyze in detail the

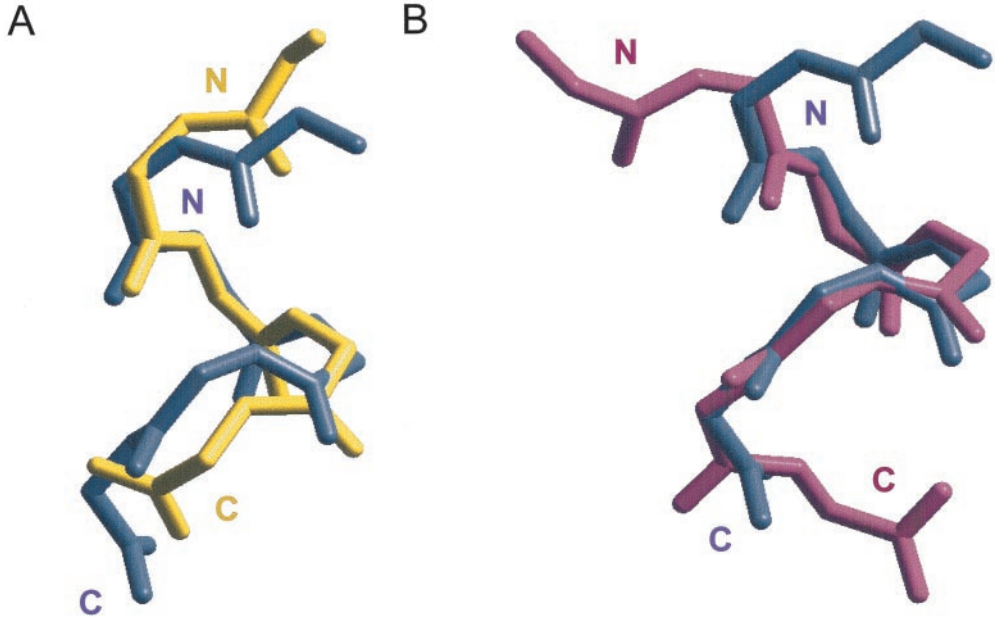


**Fig. 9.** Spatial alignment of $CGRP_{1-6}$, $_{1-5}$, or $_{1-7A}$ backbones. A, comparison of $CGRP_{1-6}$ backbone (blue) with the one of $CGRP_{1-5}$ (yellow). B, comparison of $CGRP_{1-6}$ backbone (blue) with the one of $CGRP_{1-7A}$ (magenta).

nature of the $CGRP_{1-6}$ potentiating action. Recent work, however, has indicated that the amount of agonist delivered by 10- to 50-ms puffer application closely corresponds to superfusing 20 to 100 $\mu$M nicotine (Di Angelantonio and Nistri, 2001), thus providing a relatively narrow range of agonist concentrations eliciting responses sensitive to $CGRP_{1-6}$.

Even with the interpretation constraints imposed by using nonequilibrium responses to brief pulses of nicotine, it was apparent that $CGRP_{1-6}$ preferentially potentiated small over large responses to nicotine. In fact, the graph plotting the fractional response amplitude versus the amount of nicotine showed a leftward shift (with unchanged maximum response) in the presence of $CGRP_{1-6}$. Thus, this peptide increased the sensitivity of nAChRs to their agonist nicotine without changing the agonist efficacy on them.

On muscle-type nicotinic receptors two ligand binding sites, formed at $\alpha$-$\gamma$ and $\alpha$-$\delta$ interfaces, differ in their affinities for agonists and competitive antagonists (Sine et al., 1995). On nAChRs distinct binding sites can bind certain neurotoxins that, nevertheless, share a similar mechanism of competitive antagonism (Harvey et al., 1997). It is currently unknown, on nAChRs, whether different agonists can bind to discrete sites of the receptor and activate it. It might be possible that $CGRP_{1-6}$ operated by binding to one of these sites and thus facilitated the action of the agonist nicotine. This hypothetical mode of action, however, should be considered in the light of inactivity of $CGRP_{1-6}$ alone on native nAChRs, indicating that the $CGRP_{1-6}$-sensitive site could not activate nicotinic channels in the absence of nicotine (or cytisine). This possibility will therefore require future experiments based on recombinant receptors with identified subunit binding sites.

Another possibility is that $CGRP_{1-6}$ might have acted as an APL on nAChRs (Changeux and Edelstein, 1998). When used at submicromolar concentration APLs facilitate nicotine-induced responses even if generated by desensitized receptors, whereas a 10 times higher dose depresses nAChR-mediated responses (Maelicke et al., 1997; Maelicke and Albuquerque, 2000). This property was confirmed in the present study with physostigmine, which enhanced nicotine currents at 0.5 $\mu$M and depressed them at 5 $\mu$M concentration. Note also that, for either potentiation or depression, the maximum of the nicotine dose-response curve was significantly changed, unlike the observations with CGRP derivatives, which could not increase the maximum responses and therefore could not reverse receptor desensitization associated with large membrane currents. Coapplication of enhancing concentrations of physostigmine and $CGRP_{1-6}$ led to linear summation of the individual effects, whereas $CGRP_{1-6}$ could partly reverse the depression by a large concentration of physostigmine. Taken together, these data indicate pharmacologically different effects by $CGRP_{1-6}$ and physostigmine on nicotine-induced currents and suggest functionally distinct sites of action for $CGRP_{1-6}$ and physostigmine.

**Acknowledgments**

We thank Dr. Stefano Piana for help with the annealing procedure and Dr. Andrea Cavalli for helpful discussions. We thank Dr. Massimo Righi for support with chromaffin cell cultures. We are most grateful to Prof. F. Ruzzier (Department of Physiology, University of Trieste) for laboratory facilities to perform electrophysiological experiments on I28 cells in culture, and to Drs. A. Barberis and E. Petrini (International School for Advanced Studies, Trieste, Italy) for providing a sample of transfected HEK 293 cells.

**References**

Allen MP and Tildesley DJ (1987) *Computer Simulation of Liquids*. Clarendon Press, Oxford.

Berendsen HJC, Postma JPM, Van Gunsteren WF, Di Nola A, and Haak JR (1984) Molecular dynamics with coupling to an external bath. *J Chem Phys* **81:**3684–3690.

Brandsen C and Tooze J (1993) *Introduction to Protein Structure.* Garland Publishing, New York.

Campos-Caro A, Smillie FI, Dominguez del Toro E, Rovira JC, Vicente-Agullo F, Chapuli J, Juiz JM, Sala S, Sala F, Ballesta JJ, et al. (1997) Neuronal nicotinic acetylcholine receptors on bovine chromaffin cells: cloning, expression, and genomic organization of receptor subunits. *J Neurochem* **68:**488–497.

Changeux JP and Edelstein SJ (1998) Allosteric receptors after 30 years. *Neuron* **21:**959–980.

Cornell WD, Cieplak P, Bayly CI, Gould IR, Merz KM Jr, Ferguson DM, Spellmeyer DC, Fox T, Caldwell JW, and Kollman PA (1995) A second generation force field for the simulation of proteins and nucleic acids. *J Am Chem Soc* **117:**5179–5197.

Costa JJ, Averill S, Ching YP, and Priestley JV (1994) Immunocytochemical localization of a growth-associated protein (GAP-43) in rat adrenal gland. *Cell Tissue Res* **275:**555–566.

Daura X, Jaun B, Seebach D, van Gunsteren WF, and Mark AE (1998) Reversible peptide folding in solution by molecular dynamics simulation. *J Mol Biol* **280:**925–932.

Di Angelantonio S and Nistri A (2001) Calibration of agonist concentrations applied by pressure pulses or via rapid solution exchanger. *J Neurosci Methods* **110:**155–161.

Di Angelantonio S, Nistri A, Moretti M, Clementi F, and Gotti C (2000) Antagonism of nicotinic receptors of rat chromaffin cells by *N*,*N*,*N*-trimethyl-1-(4-transstilbenoxy)-2-propylammonium iodide: a patch clamp and ligand binding study. *Br J Pharmacol* **129:**1771–1779.

Essmann U, Perera L, Berkowitz ML, Darden T, Lee H, and Pedersen LG (1995) A smooth particle mesh Ewald method. *J Chem Phys* **103:**8577–8593.

Giniatullin R, Di Angelantonio S, Marchetti C, Sokolova E, Khiroug L, and Nistri A (1999) Calcitonin gene-related peptide rapidly downregulates nicotinic receptor function and slowly raises intracellular $Ca^{2+}$ in rat chromaffin cells in vitro. *J Neurosci* **19:**2945–2953.

Giniatullin R, Khiroug L, Talantova M, and Nistri A (1996) Fading and rebound of currents induced by ATP in PC12 cells. *Br J Pharmacol* **119:**1045–1053.

Giniatullin RA, Sokolova EM, Di Angelantonio S, Skorinkin A, Talantova MV, and Nistri A (2000) Rapid relief of block by mecamylamine of neuronal nicotinic acetylcholine receptors of rat chromaffin cells in vitro: an electrophysiological and modeling study. *Mol Pharmacol* **58:**778–787.

Gotti C, Fornasari D, and Clementi F (1997) Human neuronal nicotinic receptors. *Prog Neurobiol* **53:**199–237.

Granja R, Strakhova M, Knauer CS, and Skolnick P (1998) Anomalous rectifying properties of 'diazepam-insensitive' GABA(A) receptors. *Eur J Pharmacol* **345:** 315–321

Harvey SC, Mcintosh JM, Cartier GE, Maddox FN, and Luetje CW (1997) Determinants of specificity for $\omega$-conotoxin MII on $\alpha 3\beta 2$ neuronal nicotinic receptors. *Mol Pharmacol* **51:**336–342.

Heym C, Braun B, Shuyi Y, Klimaschewski L, and Colombo-Benkmann M (1995) Immunohistochemical correlation of human adrenal nerve fibres and thoracic dorsal root neurons with special reference to substance P. *Histochem Cell Biol* **104:**233–243.

Impellizzeri G, Pappalardo G, Purrello R, Rizzarelli E, and Santoro AM (1998) Synthesis, spectroscopic characterisation, and metal ion interaction of a new alpha-helical peptide. *Chem Eur J* **4:**1791–1798

Irintchev A, Langer M, Zweyer M, Theisen R, and Wernig A (1997) Functional improvement of damaged adult mouse muscle by implantation of primary myoblasts. *J Physiol (Lond)* **500:**775–785.

Jorgensen WL, Chandrasekhar J, and Madura JD (1983) Comparison of simple potential functions for simulating liquid water. *J Chem Phys* **79:**926–935.

Khiroug L, Giniatullin R, Sokolova E, Talantova M, and Nistri A (1997) Imaging of intracellular calcium during desensitization of nicotinic acetylcholine receptors of rat chromaffin cells. *Br J Pharmacol* **122:**1323–1332.

Khiroug L, Sokolova E, Giniatullin R, Afzalov R, and Nistri A (1998) Recovery from desensitization of neuronal nicotinic acetylcholine receptors of rat chromaffin cells is modulated by intracellular calcium through distinct second messengers. *J Neurosci* **18:**2458–2466.

Krause RM, Buisson B, Bertrand S, Corringer PJ, Galzi JL, Changeux JP, and Bertrand D (1998) Ivermectin: a positive allosteric effector of the $\alpha$7 neuronal nicotinic acetylcholine receptor. *Mol Pharmacol* **53:**283–294.

Kuramoto H, Kondo H, and Fujita T (1987) Calcitonin gene-related peptide (CGRP)-like immunoreactivity in scattered chromaffin cells and nerve fibers in the adrenal gland of rats. *Cell Tissue Res* **247:**309–315.

Laskowski RA, MacArthur MW, Moss DS, and Thornton JM (1993) PROCHECK: a program to check the stereochemical quality of protein structures. *J Appl Crystallogr* **26:**283–291.

Lindstrom J (1997) Nicotinic acetylcholine receptors in health and disease. *Mol Neurobiol* **15:**193–222.

Maelicke A and Albuquerque EX (2000) Allosteric modulation of nicotinic acetylcholine receptors as a treatment strategy for Alzheimer's disease. *Eur J Pharmacol* **393:**165–170.

Maelicke A, Coban T, Storch A, Schrattenholz A, Pereira EFR, and Albuquerque EX (1997) Allosteric modulation of torpedo nicotinic acetylcholine receptor ion channel activity by noncompetitive agonists. *J Recept Signal Transduct Res* **17:**11–28.

Maltby N, Broe GA, Creasey H, Jorm AF, Christensen H, and Brooks WS (1994)

Efficacy of tacrine and lecithin in mild to moderate Alzheimer's disease: double blind trial. *Br Med J* **308:**879–883.
Moore SA, Sielecki AR, Chernaia MM, Tarasova NI, and James MN (1995) Crystal and molecular structures of human progastricsin at 1.62 A resolution. *J Mol Biol* **247:**466–485.
Nordberg A, Amberla K, Shigeta M, Lundqvist H, Viitanen M, Hellstrom-Lindahl E, Johansson M, Andersson J, Hartvig P, Lilja A, et al. (1998) Long-term tacrine treatment in three mild Alzheimer patients: effects on nicotinic receptors, cerebral blood flow, glucose metabolism, EEG, and cognitive abilities. *Alzheimer Dis Assoc Dis* **12:**228–237.
Paterson D and Nordberg A (2000) Neuronal nicotinic receptors in the human brain. *Prog Neurobiol* **61:**75–111.
Ramachandran GN and SaseikharanV (1968) Conformation of polypeptides and proteins. *Adv Protein Chem* **28:**283–438.
Reed J and Reed TA (1997) A set of constructed type spectra for the practical estimation of peptide secondary structure from circular dichroism. *Anal Biochem* **254:**36–40.
Role LW and Berg DK (1996) Nicotinic receptors in the development and modulation of CNS synapses. *Neuron* **16:**1077–1085.
Sine SM, Kreienkamp HJ, Bren N, Maeda R, and Taylor P (1995) Molecular dissection of subunit interfaces in the acetylcholine receptor: identification of determinants of alpha-conotoxin M1 selectivity. *Neuron* **15:**205–211.
Sjoberg SL, Svensson AI, Zhang X, and Nordberg A (1998) Neuronal nicotinic receptor activation: a promising strategy for treatment of Alzheimer's disease? *Int J Gerontol Psychopharmacol* **1:**145–149.
Sokolova E, Nistri A, and Giniatullin R (2001) Negative cross-talk between anionic $GABA_A$ and cationic P2X ionotropic receptors of rat dorsal root ganglion neurons. *J Neurosci* **21:**4958–4968.
Wernig A, Zweyer M, and Irintchev A (2000) Action of skeletal muscle tissue formed after myoblast transplantation into irradiated mouse muscles. *J Physiol (Lond)* **522:**333–345.

**Address correspondence to:** A. Nistri, International School for Advanced Studies, Via Beirut 4, 34014 Trieste, Italy. E-mail: nistri@sissa.it